In: Water Resources Research Progress
Editor: Liam N. Robinson, pp. 275-296
ISBN: 978-1-60021-973-3

Chapter 11

CONTINUOUS BIOSORPTION OF SINGLE AND BINARY METAL SOLUTIONS IN A FIXED-BED COLUMN USING ALGAE GELIDIUM AND GRANULATED ALGAL WASTE FROM AGAR EXTRACTION

Vítor J.P. Vilar[a1], Cidália M.S. Botelho[a2], Ramiro J.E. Martins[b3] and Rui A.R. Boaventura[a,*]

[a]LSRE-Laboratory of Separation and Reaction Engineering, Department of Chemical Engineering, Faculty of Engineering, University of Porto
Rua Dr. Roberto Frias, 4200-465 Porto, Portugal
[b]Department of Chemical and Biological Technology, Superior School of Technology, Polytechnic Institute of Bragança, Campus de Santa Apolónia
5301-857 Bragança, Portugal

Abstract

This paper describes the biosorption of single (Zn(II) and Cr(III)) and binary (Cd(II)/Zn(II) and Cu(II)/Cr(III)) metal solutions in a packed bed column using algae *Gelidium* and an algal waste from the agar extraction industry immobilized with polyacrylonitrile. In the sorption process, Zn(II) breaks through the column faster than Cd(II) due to its lower affinity for the biosorbent. An overshoot in the outlet Zn(II) concentration was observed and explained by competitive adsorption between Cd(II) and Zn(II), whereby the higher Cd(II) affinity for the biosorbent displaces bound Zn(II) ions. The same was verified for the binary system Cu(II)/Cr(III), where an overshoot in the outlet Cu(II) concentration also appeared. Metal desorption using 0.1 M HNO_3 as eluant was 100% effective for Cd(II), Zn(II) and Cd(II)/Zn(II) systems. For Cr(III) and Cu(II)/Cr(III) systems, the elution of Cr(III) was not 100% effective.

[1] E-mail address: vilar@fe.up.pt
[2] E-mail address: cbotelho@fe.up.pt
[3] E-mail address: rmartins@ipb.pt
[*] E-mail address: bventura@fe.up.pt, Tel.: +351225081683; Fax.: +351225081674 (Corresponding author)

A mathematical model for a fixed-bed system considering film and intraparticle diffusion, equilibrium represented by single and binary Langmuir equations and desorption described by the mass action law, was developed. The uptake breakthrough and elution curves obtained in fixed-bed experiments were adequately predicted by the model.

Keywords: continuous biosorption, algae, packed bed column, modelling, heavy metals

1. Introduction

Compounds of zinc(II), cadmium(II), copper(II) and chromium(III) are used in several industries, such as metal plating, mining, batteries production, leather tanning, etc. The effluents produced by these industries, containing different concentrations of metal ions, which originate negative effects on water resources. Biosorption is a wastewater treatment process capable of removing toxic metals from aqueous solutions by sorption onto low cost biomass. Different kinds of natural biomass have been used to remove toxic metals from solution, such as, bacteria [1, 2], fungi [3], blue algae [4], green algae [5], red algae [6], brown algae [7-9], peat [10], aquatic moss [11] and crushed coconut shell [12], tree fern [13], waste brewery biomass [14], etc. Red alga *Gelidium* and an algal waste from agar extraction immobilized in polyacrylonitrile have been used as biosorbents to remove Pb(II), Cu(II), Cd(II), Zn(II) and Cr(III) in a batch system at different pH, temperature and ionic strength, with the interference of other co-ions, exhibiting a good ability to remove the metal ions [15-21]. Two adsorber configurations, packed bed column and CSTR, fed with single (Cd(II), Cu(II) and Pb(II)) [15, 22] and binary solutions (Cu(II)/Pb(II) and Pb(II)/Cd(II)) [15, 23] have been tested. Better results were achieved in the packed bed column. The carboxylic groups present in the surface of the biosorbent particles, determined by potentiometric titration, are responsible by the uptake of the metal ions [15]. The affinity of the metal ions to the carboxylic groups decreases in the following sequence: Pb(II) > Cu(II) ≈ Cr(III) > Cd(II) > Zn(II) [19]. Ion exchange is the principal mechanism of biosorption, as demonstrated by the hydrogen ions released during the metal uptake [15, 22-24]. In the biosorption of multi-metal mixtures, both in a packed bed column and CSTR, metal ions compete to the same available sites, resulting in overshoots of the metal with the low affinity to the binding sites [15, 23]. In this work, a mass transfer model was used to describe the experimental breakthrough curves for adsorption and desorption experiments with good results.

The magnitude of the overshoots of Zn(II) and Cu(II), respectively in the systems Cd(II)/Zn(II) and Cu(II)/Cr(III) sorbing onto the algae *Gelidium* and the granulated algal waste, using a flow-through column, was also predicted by the model

2. Materials and Methods

2.1. Biosorbents

An algal waste from the agar extraction industry granulated with polyacrylonitrile was used in this study as well as the algae *Gelidium* itself, which is the raw material for agar extraction. The characteristics and preparation of both materials for the experimental work were presented in previous works [21, 25].

2.2. Preparation of Metal Ions Solutions

Cd(II), Zn(II), Cu(II) and Cr(III) solutions were prepared by dissolving a weighed quantity of anhydrous cadmium (II) chloride (Sigma-Aldrich, 99%), anhydrous zinc (II) chloride (Merck, 98%), copper (II) chloride dehydrate (Riedel-de Haën, 99%) and chromium (III) nitrate nonahydrate (Carlo Erba, 98%) in distilled water. Solutions pH was adjusted by adding 0.01M HCl and 0.01 M NaOH solutions.

2.3. Analytical Procedure

The concentration of Cd, Zn, Cu and Cr in aqueous solution, both in the equilibrium and dynamic study, was determined by Atomic Absorption Spectrometry (GBC 932 Plus Atomic Absorption Spectrometer). The amount of metal adsorbed per gram of biosorbent at equilibrium was calculated from the metal balance to the batch contactor.

3. Results and Discussion

3.1. Equilibrium

The equilibrium results for single (Cd^{2+}, Cu^{2+}, Zn^{2+} and Cr^{3+}) and binary (Cd^{2+}/Zn^{2+} and Cu^{2+}/Cr^{3+}) biosorption systems onto algae *Gelidium* and composite material were presented in previous works [15, 17-19]. Discrete and continuous equilibrium models successfully described the experimental data. As the continuous model is more complex, the discrete model, which can be transformed into a single or binary Langmuir equation at pH constant, was used to represent the equilibrium in the mass transfer model.

The parameters of the discrete model are [15]: Zn - Q_{max} = 0.29 ± 0.01 and 0.098 ± 0.002, pK_{Zn} = 2.9 ± 0.1 and 3.4 ± 0.1, pK_{Cr} = 3.1 ± 0.1 and 4.1 ± 0.1, pK_H = 4.2 ± 0.1 and 5.6 ± 0.1, respectively for algae *Gelidium* and composite material; Cd/Zn - Q_{max} = 0.26 ± 0.02 and 0.097 ± 0.004, pK_{Cd} = 3.2 ± 0.1 and 3.4 ± 0.1, pK_{Zn} = 3.0 ± 0.1 and 3.4 ± 0.1, pK_H = 4.2 ± 0.1 and 4.4 ± 0.1, respectively for algae *Gelidium* and composite material; Cu/Cr - Q_{max} = 0.41 ± 0.02 and 0.165 ± 0.004, pK_{Cu} = 3.1 ± 0.1 and 4.3 ± 0.1, pK_{Cr} = 3.1 ± 0.1 and 4.1 ± 0.1, pK_H = 4.2 ± 0.1 and 5.6 ± 0.1, respectively for algae *Gelidium* and composite material. These parameters were obtained, considering the results from the single-metal systems at pH 5.3, 4 and 3 for Cu(II), 6.5, 5.3 and 4 for Cd(II), 5.3 for Zn(II) and Cr(II) ions and the binary systems (Cd(II)/Zn(II) and Cu(II)/Cr(II)) at pH 5.3.

Table 1. Operation parameters for the breakthrough and elution curves.

Material	Metal	Type	Q (cm^3 min^{-1})	pH_{SE}	pH_{CI}	pH_{CE}	C_{Ei} / C_{CI} (mg l^{-1})	$C_{final(i)}$(mg l^{-1})	W (g)	ε	τ (min)
Gelidium	Zn	S	4.0	5.3	5.3	4.9	45.6 / 0	43.0	10.7	0.891	16.4
		E	8.0	0.9	4.9	0.9	0 / 43.0	< 0.03	10.7	0.891	8.2
	Cr	S	4.0	5.1	5.5	4.0	48.2 / 0	41.0	10.0	0.899	16.5
		E	7.8	0.93	4.0	0.93	0 / 41.0	12.4	10.0	0.899	8.5
	Cd/Zn	S	4.0	5.4	5.2	4.5	Cd– 47.8 / 0; Zn – 51.5 / 0	Cd – 48.0; Zn – 51.0	10.0	0.899	16.5
		E	7.8	0.78	4.4	0.78	Cd – 0 / 53.0; Zn – 0 / 56.0	Cd – 0.01; Zn – 0.01	10.0	0.899	8.5
	Cu/Cr	S	4.1	5.0	5.4	4.1	Cu – 49.8 / 0; Cr – 48.8 / 0	Cu – 53.0; Cr – 29.0	10.6	0.893	16.0
		E	8.0	0.72	4.1	0.72	Cu – 0 / 52.5; Cr – 0 / 27.3	Cu – 0.3; Cr – 22.0	10.6	0.893	8.2
Composite material	Zn	S	4.1	5.2	5.2	4.7	46.5 / 0	44.0	9.3	0.493	8.9
		E	8.0	0.89	4.7	0.89	0 / 42.0	0.1	9.3	0.493	4.5
	Cr	S	4.0	5.1	5.4	4.2	45.5 / 0	41.9	9.6	0.478	8.8
		E	8.0	0.9	4.2	0.9	0 / 41.9	2.1	9.6	0.478	4.4
	Cd/Zn	S	4.0	5.3	5.6	5.0	Cd– 46.2 / 0; Zn – 48.4 / 0	Cd – 47.0; Zn – 49.0	8.3	0.546	10.1
		E	8.0	0.73	5.0	0.73	Cd – 0 / 43.6; Zn – 0 / 45.9	Cd – < 0.01; Zn – < 0.01	8.3	0.546	5.0
	Cu/Cr	S	4.0	5.0	5.8	4.1	Cu – 49.1 / 0; Cr – 48.0 / 0	Cu – 49.1; Cr – 36.2	9.2	0.497	9.2
		E	7.8	0.72	4.1	0.72	Cu – 0 / 49.6; Cr – 0 / 49.8	Cu – 0.08; Cr – 2.0	9.2	0.497	4.7

*S – Saturation; E – Elution

3.2. Continuous Biosorption

The operation parameters used for each continuous experiment are presented in Table 1. The biosorption of zinc and chromium ions by algae *Gelidium* and algal waste immobilized in polyacrylonitrile was studied in a packed bed column. Figs. 1 and 2 show the breakthrough curves for the two metal ions and the pH profiles. The flow rate was set at 4 ml min^{-1}, and the inlet metal concentration was approximately 50 mg l^{-1}. The breakthrough time is higher for chromium than for zinc for both biosorbents, suggesting that chromium ions have a higher affinity to the binding sites at the same operating conditions. It can be also noticed (Table 1) that MTZ and LUB show the same tendency. The difference between the initial and final pH is higher for Cr biosorption, as more Cr ions were bound to the carboxylic groups and consequently more hydrogen ions were displaced. In order to predict the experimental breakthrough curves, a mass transfer model for the biosorption process was developed assuming isothermal operation, axial dispersed plug flow of the fluid phase, adsorption equilibrium described by the extended Langmuir isotherm, external (film) resistance to mass transfer and internal mass transfer resistance described by the LDF approximation:

Mass conservation in the fluid around particles:

$$\frac{\partial y_{b_i}(x,\theta)}{\partial \theta} = \frac{1}{Pe}\frac{\partial^2 y_{b_i}(x,\theta)}{\partial x^2} - \frac{\partial y_{b_i}(x,\theta)}{\partial x} - \xi_i \; N_{d_i}\left[y_i^*(x,\theta) - \langle y_i(x,\theta)\rangle\right] \tag{1}$$

Mass conservation inside particles (LDF-Linear Driving Force):

$$\frac{d\langle y_i(x,\theta)\rangle}{d\theta} = N_{d_i}\left[y_i^*(x,\theta) - \langle y_i(x,\theta)\rangle\right] \tag{2}$$

where $k_{p_i}\; a_p = 3\, D_{h_i} / R^2$, considering a parabolic profile of the metal concentration inside the particle and $a_p = 1/R$ the specific area for thin plate particles.

For a situation of no accumulation in the fluid film surrounding the particles, we can write:

$$\frac{d\langle y_i(x,\theta)\rangle}{d\theta} = \frac{N_{f_i}}{\xi_i}\left[y_{b_i}(x,\theta) - y_{f_i}(x,\theta)\right] \tag{3}$$

Extended Langmuir equation:

$$q_{M_i} = \frac{Q_{max}\; K_i\; C_{M_i}}{1 + \sum_{i=1}^{n} K_i\; C_{M_i}} \tag{4}$$

Initial and boundary conditions:

$$\theta = 0 \qquad y_{b_i}(x,0) = y_{f_i}(x,0) = \langle y_i(x,0) \rangle = 0 \tag{5}$$

$$x = 0 \qquad -\frac{1}{Pe}\frac{\partial\, y_{b_i}(x,\theta)}{\partial x} + y_{b_i}(x,\theta) = 1 \tag{6}$$

$$x = 1 \qquad \left.\frac{\partial\, y_{b_i}(x,\theta)}{\partial x}\right|_{x=1} = 0 \tag{7}$$

Dimensionless variables:

$$x = \frac{z}{L},\ \theta = \frac{t}{\tau},$$
$$y_{b_i}(x,\theta) = \frac{C_{b_i}(z,t)}{C_{E_i}},$$
$$y_{f_i}(x,\theta) = \frac{C_{f_i}(z,t)}{C_{E_i}},$$
$$\langle y_i(x,\theta) \rangle = \frac{\langle q_i(z,t) \rangle}{Q_{max}},$$
$$y_i^*(x,\theta) = \frac{q_i^*(z,t)}{Q_{max}},$$
$$\tau = \frac{\varepsilon\, L}{u_i},\ \tau_{d_i} = \frac{R^2}{D_{h_i}},$$
$$\tau_{d_i}^* = \frac{1}{k_{p_i} a_p} = \frac{\tau_{d_i}}{3},$$
$$\tau_{f_i} = \frac{\varepsilon}{(1-\varepsilon)}\frac{1}{k_{f_i}\ a_p} \tag{8}$$

Dimensionless parameters:

$$\xi_i = \frac{(1-\varepsilon)}{\varepsilon}\rho_{ap}\frac{Q_{max}}{C_{E_i}},$$
$$N_{f_i} = \frac{\tau}{\tau_{f_i}} = \frac{(1-\varepsilon)}{\varepsilon} k_{f_i}\ a_p\ \tau,\ N_{d_i} = \frac{\tau}{\tau_{d_i}^*} = k_{p_i} a_p \tau,$$

$$Pe = \frac{u_i \, L}{D_{ax}} \tag{9}$$

The partial differential Eq. (1) combined with Eq. (2) and Eq. (3), in conjunction with the initial (Eq. 5) and boundary conditions (Eqs. 6 and 7) for each metal ion, were solved by the FORSIM *package* [26], where equilibrium was given by the extended Langmuir isotherm.

The models parameters (mass, inlet concentration, porosity, time residence, equilibrium pH and others) are presented in Table 1. The homogeneous diffusion coefficient, D_h, was determined from a batch dynamic study (D_h = 4.8×10^{-8} and 6.2×10^{-8} cm^2 s^{-1} for Zn, D_h = 4.2×10^{-8} and 1.4×10^{-8} cm^2 s^{-1} for Cr, respectively for algae *Gelidium* and composite material).

As the Peclet number based on the particle diameter [27] is high, the axial dispersion is negligible. Nevertheless, the axial dispersion was included in the model.

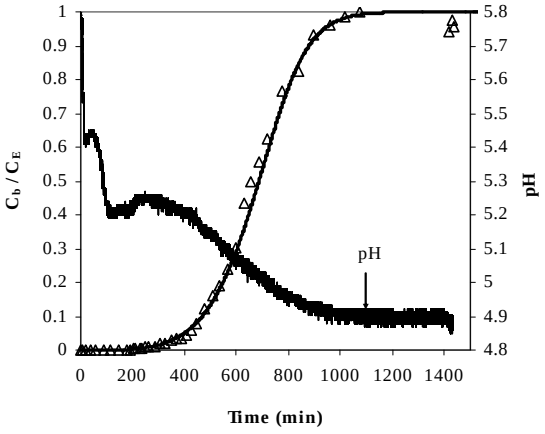

(a)

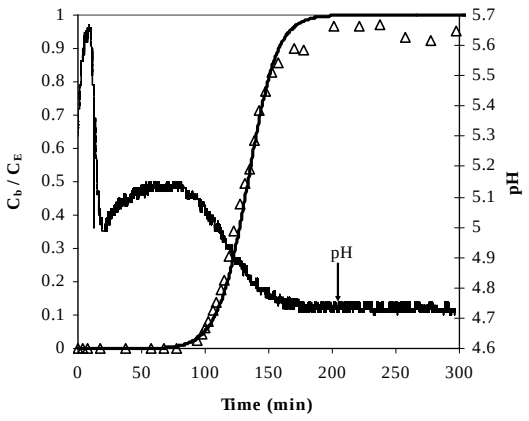

(b)

Figure 1. Comparison between the experimental and mass transfer model calculated breakthrough curves for zinc: (a) – algae *Gelidium*, (b) -composite material.

As observed for Cu(II), the equilibrium uptake capacity of Cr(III) and Zn(II) by algae *Gelidium* is higher in the packed bed column than in the batch system, due to competition between dissolved organics released by the biosorbent and the sites at the particles surface to bind the metal ions, decreasing the biosorption capacity. To obtain a better fitting of the mass transfer model to the experimental data, the maximum uptake capacity was increased (Fig. 1a and Fig. 2a). However, for the composite material, the content of dissolved organics in the batch operation mode is very low and the model reasonably predicts the data (Fig. 1b and Fig. 2b).

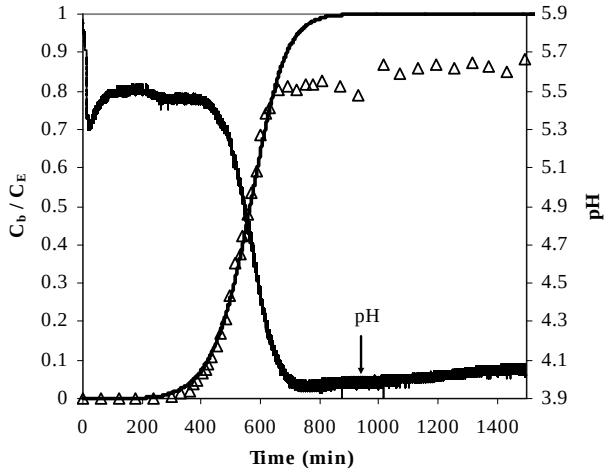

(a)

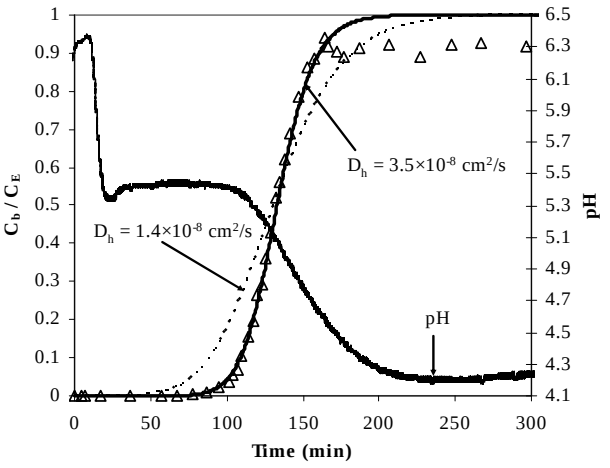

(b)

Figure 2. Comparison between the experimental and mass transfer model calculated breakthrough curves for chromium: (a) – algae *Gelidium*, (b) -composite material.

For the algae *Gelidium*, $\xi_i N_{d_i} >> N_{f_i}$, so we can conclude that the process is external mass transfer controlled. In the case of the composite material, $\xi_i N_{d_i} < N_{f_i}$, which proves that the intraparticle resistance has a higher contribution to the sorption mechanism.

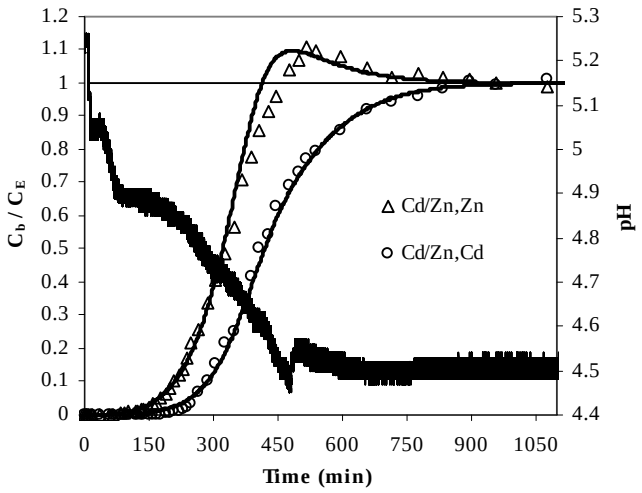

(a)

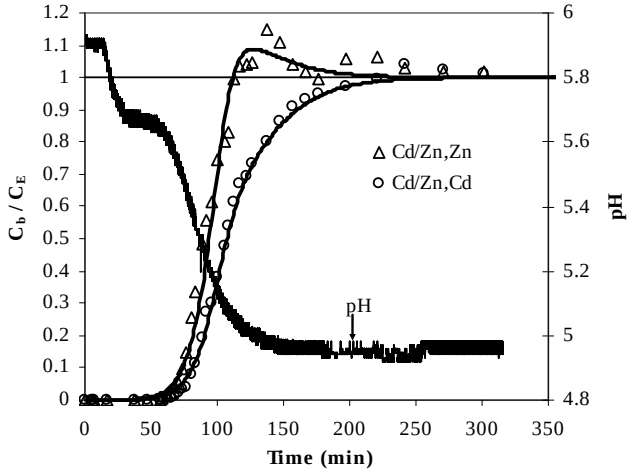

(b)

Figure 3. Comparison between the experimental and mass transfer model calculated breakthrough curves for Cd/Zn: (a) – algae *Gelidium*, (b) -composite material.

Fig. 3 (a) and (b) shows the breakthrough curves for metal adsorption from the binary Cd(II)/Zn(II) solution ($C_E \approx 0.42$ mmol l^{-1} for Cd and ≈ 0.76 mmol l^{-1} for Zn), respectively for the algae *Gelidium* and the composite material. Zinc breaks through the column faster than Cd and a small overshoot is observed for Zn, suggesting competition between Cd and Zn for the same binding sites. The higher biosorbent affinity of Cd (K_{Cd}/K_{Zn} = 1.6 for the algae and 1.3 for the composite material) causes the Zn displacement from the biosorbent surface, despite the higher feed concentration of Zn ($C_E(Cd)/C_E(Zn) \approx$ 1.8). The mass transfer model parameters are presented in Table 3, indicating that the process is external mass transfer controlled.

Table 2. **Mass transfer parameters for biosorption of Zn and Cr.**

Metal	K_M (l mg^{-1})	Q_{max}(mg g^{-1})	ξ_i	ε	k_{f_i} (cm s^{-1})	N_{d_i}	$\xi_i N_{d_i}$	N_{f_i}	t_{st} (min)	t_{Bp} (min)	MTZ (cm)	LUB (%)
Zn[a]	1.4×10^{-2}	20	27.9	0.893	5.5×10^{-4}	5.7	159.0	13.2				
		29	40.4				230.3		690.8	263	18.6	61.9
Cr[a]	1.42×10^{-2}	22	28.6	0.899	8.0×10^{-4}	5.0	143.0	17.9				
		26	32.8				164.0		557.4	330	12.2	40.8
Zn[b]	1.5×10^{-2}	6.2	14.0	0.493	3.0×10^{-4}	4.0	56.0	32.8	131.7	79	12.0	40.0
Cr[b]	8.8×10^{-3}	8.3	14.2	0.478	5.0×10^{-3}	2.0	31.5	576.5	133.9	87	10.5	35.0
						0.89	12.6					

[a] *Gelidium*: Zn*-Q_{max} = 19 ± 1 mg g^{-1}, K_{Zn} = 0.011 ± 0.003 l mg^{-1} (pH$_{CE}$ = 4.9); Cr*-Q_{max} = 21 ± 1 mg g^{-1}, K_{Cr} = 0.011 ± 0.003 l mg^{-1} (pH$_{CE}$ = 4.0); [b]Composite material: Zn*-Q_{max} = 6.4 ± 0.2 mg g^{-1}, K_{Zn} = 0.021 ± 0.006 l mg^{-1} (pH$_{CE}$ = 4.7); Cr*-Q_{max} = 8.6 ± 0.3 mg g^{-1}, K_{Cr} = 0.009 ± 0.003 l mg^{-1} (pH$_{CE}$ = 4.1).

[*] The equilibrium data for Zn and Cr were obtained from the discrete model for Pb(II)/Zn(II) and Cu(II)/Cr(III) systems, respectively.

Table 3. **Mass transfer parameters for biosorption of the binary system Cd/Zn.**

	Metal	K_M (l mmol^{-1})	Q_{max}(mmol g^{-1})	ξ_i	ε	k_{f_i} (cm s^{-1})	N_{d_i}	$\xi_i N_{d_i}$	N_{f_i}	t_{st} (min)	t_{Bp} (min)	MTZ (cm)	LUB (%)
[a]	Cd	1.1	0.28	99.5	0.899	4.5×10^{-4}	8.2	815.9	10.1	419	286	9.5	31.7
	Zn	0.7		53.7		4.0×10^{-4}		440.3	8.9	323	210	10.5	35.0
[b]	Cd	2.0	0.075	37.6	0.547	1.5×10^{-4}	2.2	82.7	15.0	106	67	11.0	36.8
	Zn	1.5		20.9		1.5×10^{-4}	5.0	104.5		90	60	10.0	33.3

[a] *Gelidium*: Q_{max} = 0.26 ± 0.02 mmol g^{-1}, K_{Cd} = 1.1 ± 0.3 l mmol^{-1} (pH$_{CE}$ = 4.5), K_{Zn} = 0.7 ± 0.2 l mmol^{-1} (pH$_{CE}$ = 4.5); [b]Composite material: Q_{max} = 0.097 ± 0.004 mmol g^{-1}, K_{Cd} = 3.3 ± 0.8 l mmol^{-1} (pH$_{CE}$ = 4.9), K_{Zn} = 3.3 ± 0.8 l mmol^{-1} (pH$_{CE}$ = 4.9).

Figueira et al. [28] studied the biosorption of Cd/Zn mixture by the algae *Sargassum* and also observed an overshoot of Zn exit concentration. The fact was explained by ion exchange between Cd and Zn, whereby the higher-affinity Cd (K_{Cd}/K_{Zn} =1.9) in solution displaces Zn already bound to the biosorbent, for the same initial concentration of each metal (1.5 meq/l).

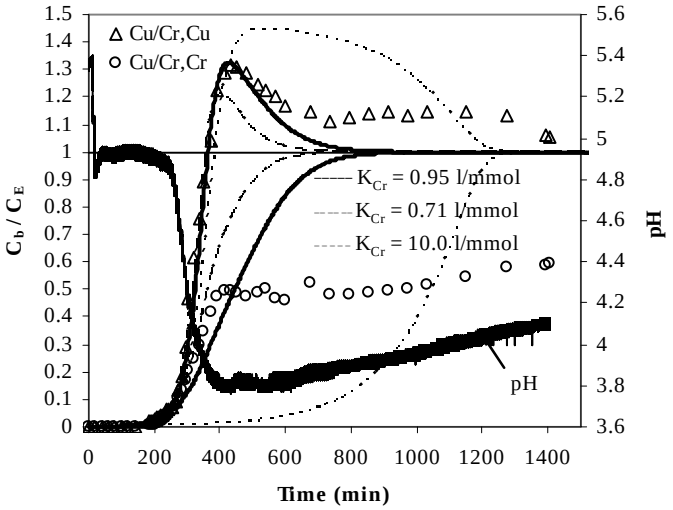

(a)

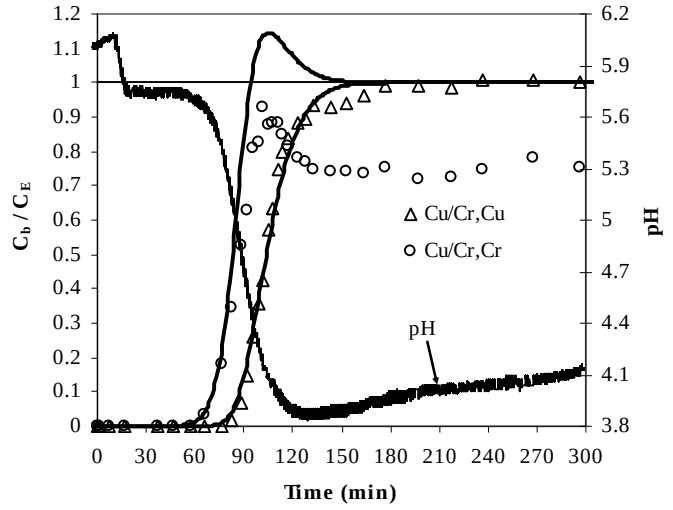

(b)

Figure 4. Comparison between the experimental and mass transfer model calculated breakthrough curves for Cu/Cr: (a) – algae *Gelidium*, (b) -composite material.

Table 4. **Mass transfer parameters for biosorption of the binary system Cu/Cr.**

	Metal	K_M (l mmol^{-1})	Q_{max}(mmol g^{-1})	ξ_i	ε	k_{f_i} (cm s^{-1})	N_{d_i}	$\xi_i N_{d_i}$	N_{f_i}	t_{st} (min)	t_{Bp} (min)	MTZ (cm)	LUB (%)
[a]	Cu	0.52	0.41	84.9	0.893	1.0×10^{-3}	32.3	2745	23.1	230	180	6.5	21.7
	Cr	0.95		70.9		4.0×10^{-4}	9.2	655	9.3	973	203	23.7	79.1
	Cu	0.52		84.9	0.893	1.0×10^{-3}	32.3	2745	23.1				
	Cr	0.71		70.9		6.0×10^{-4}	9.2	655	13.9				
	Cu	0.52		84.9	0.893	1.0×10^{-3}	32.3	2745	23.1				
	Cr	10.0		70.9		3.0×10^{-4}	9.2	655	6.9				
[b]	Cu	0.42	0.165	52.1	0.497	3.0×10^{-3}	4.6	237	333.3	103	75	8.2	27.2
	Cr	0.30		43.7		2.0×10^{-3}		199	222.2	86	60	9.1	30.2

[a]*Gelidium*: Q_{max} = 0.41 ± 0.02 mmol g^{-1}, K_{Cu} = 0.6 ± 0.2 l mmol^{-1}, K_{Cr} = 0.6 ± 0.2 l mmol^{-1} (pH_{CE} = 4.1); [b]Composite material: Q_{max} = 0.165 ± 0.004 mmol g^{-1}, K_{Cu} = 0.6 ± 0.2 l mmol^{-1}, K_{Cr} = 0.4 ± 0.1 l mmol^{-1} (pH_{CE} = 4.1).

Fig. 4 (a) and (b) displays the breakthrough curves for metal adsorption from the binary Cu(II)/Cr(III) solution ($C_E \approx 0.78$ mmol l^{-1} for Cu and ≈ 0.94 mmol l^{-1} for Cr), respectively for the algae *Gelidium* and the composite material. For *Gelidium,* the initial part of the breakthrough curve is similar for both cations, and the breakthrough time is approximately the same. After 270 min a separation occurs, and the Cu breakthrough curve reaches rapidly the feed concentration, and an overshoot region is observed, while the Cr concentration remains constant. Initially Cu(II) and Cr(III) are bound to the sites for which they have a higher affinity. When the sites become almost saturated, the concentration fronts of Cu(II) and Cr(III) reach the exit of the column. After this moment, Cr(III) competes with Cu(II) for the same binding sites, then resulting an overshoot of Cu(II) caused by the higher affinity of Cr(III) to the binding sites (K_{Cr}/K_{Cu} =1.4). When the sorbent is the composite material (Fig. 4b), the breakthrough time is lower for Cr than for Cu, which is in agreement with the affinity constants. The Cr breakthrough curve is very sharp and reaches C_b/C_E =0.93 at 102 min. Then the concentration decreases and remains below the inlet concentration, which suggests that some active sites may have a lower affinity for Cr(III), and are only occupied after the others, and/or some chromium speciation exists. This is the reason why the mass transfer model, even using different values of K_M for Cr (Table 4), was unable to predict the experimental results.

If the biosorption process is to be used as an alternative in wastewater treatment, the regeneration of the biosorbent may be crucially important to keeping the processing costs down and to opening the possibility of recovering the metal(s) extracted from the liquid phase [29]. In a previous work we concluded that the desorption of Cu (II) could be achieved with a relatively inexpensive acid such as HNO_3 [24]. Desorption was considered as ion exchange process, where the metal ions are released to the solution by exchange with the protons. The exchange rate was determined as approximately stoichiometric (1:1). Equilibrium desorption was well described by the mass action law [24]:

$$y_i^* = \frac{K_H^M \; y_{b_i}(x,\theta)}{y_T + \left(K_H^M - 1\right) y_{b_i}(x,\theta)} \tag{10}$$

where K_H^M and Q_{max} values are 0.93 and 1.1 and 0.36 and 0.16 mmol g^{-1}, respectively for the algae *Gelidium* and the composite material.

An elution model, based on the same assumptions as for the saturation model, except for the equilibrium, which is now described by the mass action law, was developed. The equilibrium is equal for both metal ions, supposing that elution of one metal does not interfere with the elution of the other metal, and considering the same value of K_H^M for both metals. So, Eqs. (1), (2) and (3) are still valid using mmol instead of mg for the concentrations.

Total mass conservation in the fluid around particles:

$$\frac{\partial y_T(x,\theta)}{\partial \theta} = \frac{1}{Pe}\frac{\partial^2 y_T(x,\theta)}{\partial x^2} - \frac{\partial y_T(x,\theta)}{\partial x} \tag{11}$$

Initial and boundary conditions:

$$\theta = 0 \quad y_{b_i}(x,0) = \frac{C_{b_{0_i}}}{C_{T_0}} \quad y_{f_i}(x,0) = \frac{C_{b_{0_i}}}{C_{T_0}} \quad y_T = 1 \quad \langle y_i(x,0) \rangle = \frac{q_{0_i}}{Q_{max}} \tag{12}$$

$$x = 0 \qquad -\frac{1}{Pe}\frac{\partial y_{b_i}(x,\theta)}{\partial x} + y_{b_i}(x,\theta) = 0 \tag{13}$$

$$-\frac{1}{Pe}\frac{\partial y_T(x,\theta)}{\partial x} + y_T(x,\theta) = \frac{C_{T_E}}{C_{T_0}} \tag{14}$$

$$x = 1 \qquad \left.\frac{\partial y_{b_i}(x,\theta)}{\partial x}\right|_{x=1} = \left.\frac{\partial y_T(x,\theta)}{\partial x}\right|_{x=1} = 0 \tag{15}$$

Dimensionless variables:

$$x = \frac{z}{L},\ \theta = \frac{t}{\tau},\ y_{b_i}(x,\theta) = \frac{C_{b_i}(z,t)}{C_{T_0}},\ y_{f_i}(x,\theta) = \frac{C_{f_i}(z,t)}{C_{T_0}},\ y_T(x,\theta) = \frac{C_T(z,t)}{C_{T_0}},$$
$$\langle y_i(x,\theta) \rangle = \frac{\langle q_i(z,t) \rangle}{Q_{max}},\ y_i^*(x,\theta) = \frac{q_i^*(z,t)}{Q_{max}} \tag{16}$$

The dimensionless parameters are the same as before, with the exception of the column capacity factor, which is now defined as:

$$\xi' = \frac{(1-\varepsilon)}{\varepsilon}\rho_{ap}\frac{Q_{max}}{C_{T_0}} \tag{17}$$

where C_{T_E} is the molar concentration of the feed solution (0.1 M HNO_3) and C_{T_0} is the sum of the metals and proton concentrations in the interstitial fluid into the column after the saturation process.

The partial differential equations (Eqs. 1 and 11) combined with Eqs. (2) and (3) for each metal ion, in conjunction with the initial (Eq. 12) and boundary conditions (Eqs. 13, 14 and 15), were solved by the FORSIM *package*, and the equilibrium was given by the mass action law (Eq. 10).

The homogeneous diffusion coefficient for desorption, D_h, was determined from a batch dynamic study (D_h = 1.0×10^{-7} and 3.0×10^{-7} $cm^2\ s^{-1}$, respectively for algae *Gelidium* and composite material) [24].

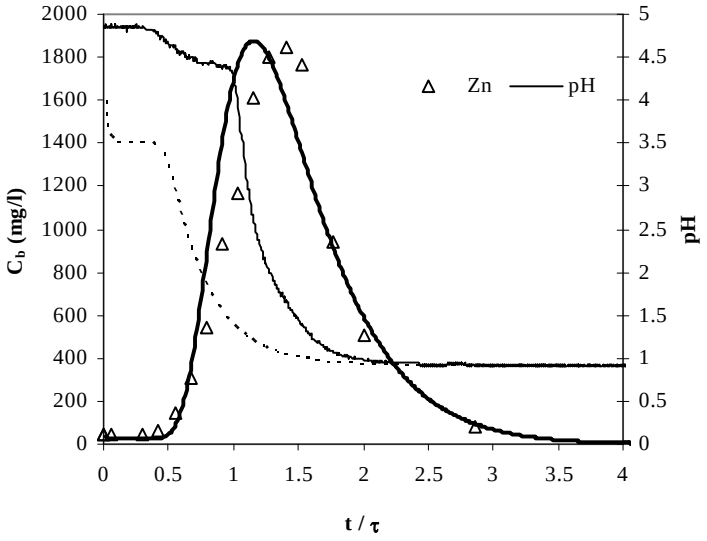

(a)

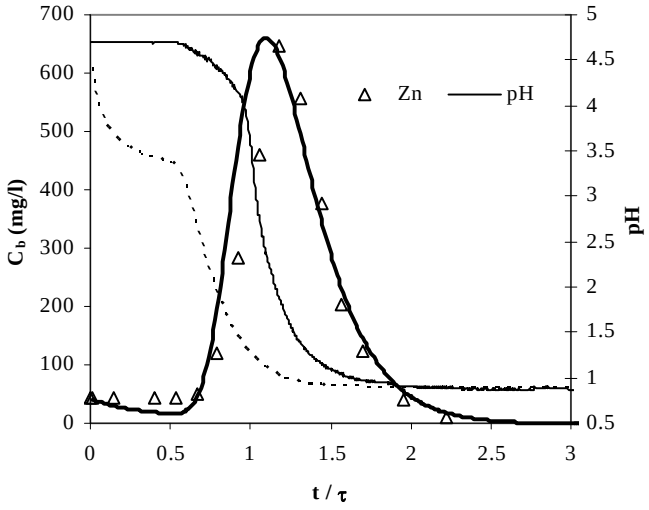

(b)

Figure 5. Comparison between the experimental and mass transfer model calculated elution curve for Zn: (a) - algae *Gelidium*, (b) - composite material.

Fig. 5 (a) and (b) shows the elution curves for zinc, as well as the pH profile. Desorption of Zn(II) occurs in a rapid and efficient way, and the curves predicted by the model are in good agreement with the experimental results. As observed in the saturation process, the particle mass transfer resistance is lower than the film resistance ($\xi' N_{d_i} >> N_{f_i}$, see Table 5), which means that intraparticle metal ions diffusion is fast and results in ion exchange with the high diffusivity protons. So, the elution process is controlled by metal ions diffusion in the film. The pH profiles indicate that elution is an ion exchange process.

Table 5. **Mass transfer parameters for desorption of Zn.**

	K_H^M	Q_{max}(mmol g^{-1})	ξ'	ε	P_e	k_{f_i} (cm s^{-1})	N_{d_i}	$\xi' N_{d_i}$	N_{f_i}
Gelidium	0.93	0.36	87.5	0.892	25	3.0×10^{-3}	4.90	429.2	36.0
Composite material	1.1	0.16	36.4	0.838	50	2.0×10^{-4}	11.7	424.1	3.6

Only 30%-40% of the Cr bound to the biomass was desorbed (Fig. 6), suggesting that a higher HNO_3 concentration was required to remove all loaded chromium. Tobin and Roux [30] found similar results for chromium desorption from *Mucor* saturated biomass. However, they observed that increasing the acid concentration up to 5 M, the desorption efficiency increased to 80% for 40 mg Cr(III) g^{-1} loaded biomass.

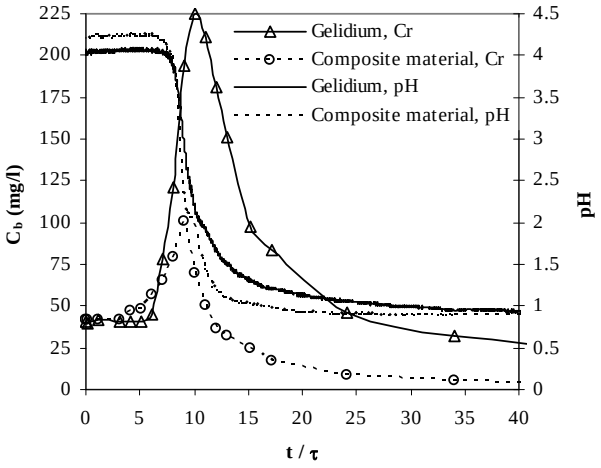

Figure 6. Experimental chromium elution curve.

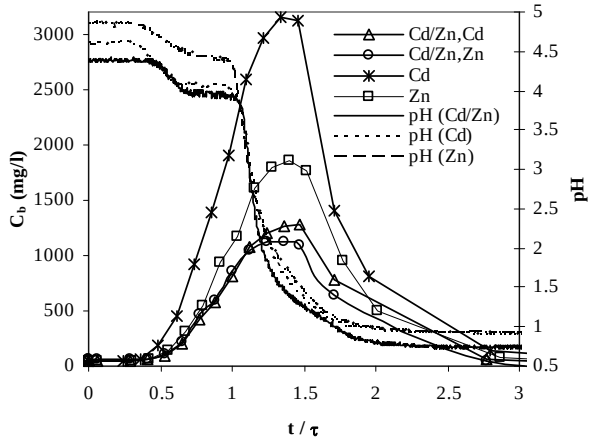

(a)

Figure 7. Continued on next page.

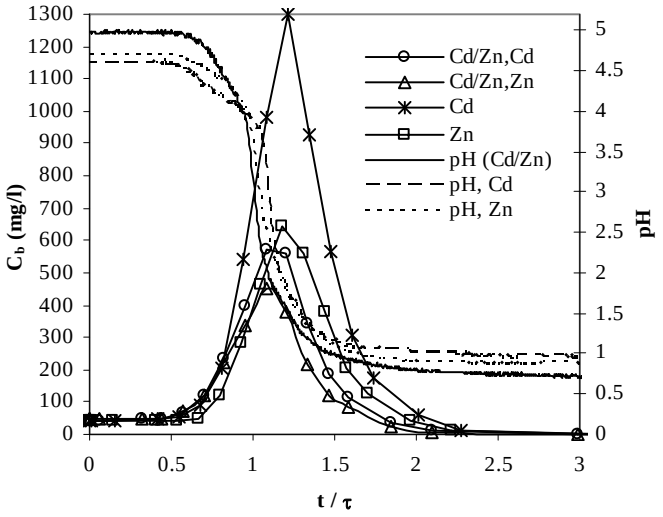

(b)

Figure 7. Comparison of experimental Cd, Zn and Cd/Zn elution curves: (a) - algae *Gelidium*, (b) - composite material.

The elution curves for single and binary sorption systems (Figs. 7 and 8) show that desorption of Cd, Zn and Cu is 100% efficient and fast. The presence of other ions does not interfere in the desorption mechanism using 0.1 M HNO_3 as eluant. The maximum concentration is lower for the binary systems than for the single system, as it is proportional to the amount of metal initially loaded in the biomass. Chromium desorption is incomplete both in single and binary systems, and further investigation is necessary.

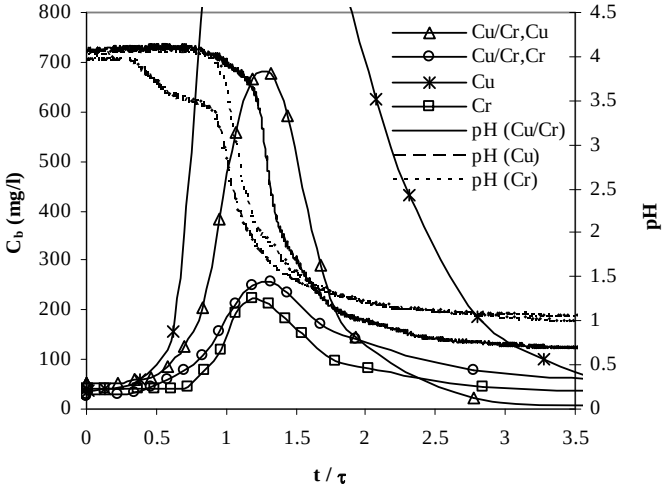

(a)

Figure 8. Continued on next page.

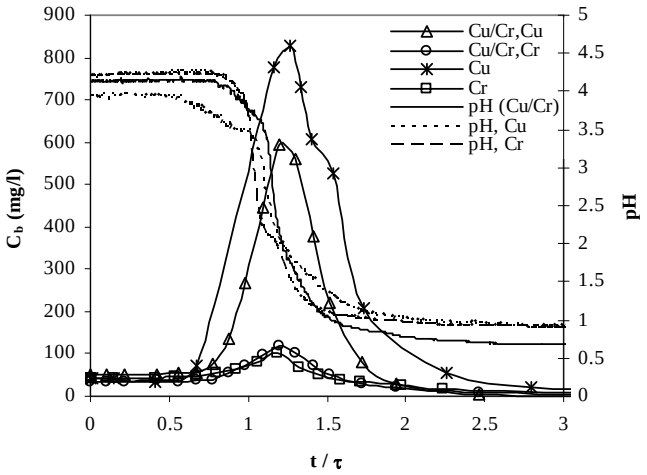

(b)

Figure 8. Comparison of experimental Cu, Cr and Cu/Cr elution curves: (a) - algae *Gelidium* and (b) - composite material.

5. Conclusions

The algae *Gelidium* and a granulated algal waste from the agar extraction industry proved to be efficient sorbents for the removal of Zn(II), Cr(III), Cd(II)/Zn(II) and Cu(II)/Cr(III) in a packed bed column. Biosorption experimental data for the binary mixtures Cd(II)/Zn(II) and Cu(II)/Cr(III) showed a higher affinity of the binding sites for Cd(II) than for Zn(II) and for Cr(III) than for Cu(II). Sorption and desorption mass transfer models were developed as a tool for the design of continuous processes in packed bed adsorbers. These models were able to predict the experimental data both for single and binary systems. The pH breakthrough curve can be used as an indicator of the metal breakthrough. Desorption with 0.1 M HNO_3 was 100% efficient except for Cr(III).

Acknowledgements

Financial support for this work was in part provided by national research grant FCT/POCTI/AMB/57616/2004 and by LSRE financing by FEDER/POCI/2010, for which the authors are thankful. V. Vilar's acknowledges his Ph.D. scholarship by FCT (SFRH/BD/7054/2001).

Nomenclature

a_p	specific area for thin plates particles (cm^{-1});
C_{b_i}	concentration in the bulk of metal *i* (mg or mmol metal/ l fluid);

$C_{b_{i_o}}$	initial concentration in the bulk of metal *i* (mg or mmol metal/ l fluid);
C_{CI}	metal concentration in the bulk solution at the beginning of the elution process (mg metal/ l fluid);
C_{E_i}	feed concentration for metal *i* (mg or mmol metal/ l fluid);
C_{f_i}	concentration in the film for metal *i* (mg or mmol metal/ l fluid);
$C_{final(i)}$	metal concentration in the solution at the end of the saturation or elution process (mg or mmol metal/ l fluid);
C_H	equilibrium concentration of proton in the fluid phase (mmol proton/l fluid);
C_{M_i}	equilibrium concentration of metal *i* in the fluid phase (mmol metal/l fluid);
C_T	total (metals + protons) liquid concentration (mmol/l fluid);
C_{T_0}	initial total (metals + protons) liquid concentration (mmol/l fluid);
C_{T_E}	total feed (eluant concentration) liquid concentration (mmol/l fluid);
d_p	particle diameter (cm);
D_{ax}	axial dispersion coefficient (cm/s);
D_{h_i}	homogeneous diffusion coefficient for metal *i* (cm^2/s);
k_{f_i}	film mass transfer coefficient for metal *i* (cm/s);
k_{p_i}	mass transfer coefficient for intraparticle diffusion for metal *i* (cm/s);
K_H	equilibrium proton constant (l fluid/ mmol H);
K_{M_i}	equilibrium metal *i* constant (l fluid/ mmol M);
K_i	equilibrium constant of Langmuir for metal *i* (l fluid/mg M);
K_H^M	selectivity coefficient between ion M in the particle and H in solution;
L	bed length (cm);
N_{d_i}	number of mass transfer units by intraparticle diffusion for metal *i*;
N_{f_i}	number of mass transfer units by film diffusion for metal *i*;
pH_{SE}	pH of feed solution;
pH_{CI}	initial pH of interstitial fluid inside the column;
pH_{CF}	final pH of interstitial fluid inside the column;
Pe	axial Peclet number based on the bed length;

$\langle q_i \rangle$	average metal *i* concentration in the solid phase (mg or mmol metal/g biomass);
q_H	equilibrium concentration of proton in the biomass (mmol metal/g biomass);
q_{M_i}	equilibrium concentration of metal *i* in the biomass (mg or mmol metal/g biomass);
q_{i_0}	metal *i* concentration in the solid phase after biomass saturation (mmol metal/g biomass);
q_i^*	solid phase concentration in equilibrium with C_{f_i} for each metal *i* (mg or mmol metal/g biomass);
Q	flow rate (cm^3/min);
Q_{max}	concentration of carboxylic groups or maximum capacity of biomass (mg or mmol/g biomass);
R	half of thickness of the thin plate (cm);
t	time (s);
t_b	breakthrough time (s);
t_{st}	stoichiometric time (s);
T	temperature (ºC);
u_i	interstitial fluid velocity (cm/s);
x	axial position normalized by the bed length;
$\langle y_i \rangle$	dimensionless average concentration in the solid phase for metal *i*;
y_{b_i}	dimensionless concentration in the fluid phase for metal *i*;
y_{f_i}	dimensionless concentration in the fluid phase at the film for metal *i*;
y_T	dimensionless total concentration in the fluid phase;
y_i^*	dimensionless concentration in the solid phase at the particle surface for metal *i*;
z	bed axial position (cm);
W	mass of biosorbent (g);
ε	adsorber porosity;
τ	space time (s);
τ_{d_i}	time constant for intraparticle diffusion for metal *i*;
τ_{f_i}	time constant for film diffusion for metal *i*;
θ	dimensionless time;
ρ_{ap}	apparent density of particles (g solid /cm^3 particle);
ξ_i	adsorber capacity factor for each metal *i* for saturation ;

ξ'	adsorber capacity factor for desorption;

References

[1] P.G. Wightman, J.B. Fein, Ternary interactions in a humic acid-Cd-bacteria system, *Chem. Geol*. **180** (2001) 55-65.

[2] N. Rangsayatorn, E.S. Upatham, M. Kruatrachue, P. Pokethitiyook, G.R. Lanza, Phytoremediation potential of *Spirulina* (*arthrospira*) *platensis*: Biosorption and toxicity studies of cadmium, *Environ. Pollut*. **119** (2002) 45-53.

[3] A. Kapoor, R. Viraraghavan, Removal of heavy metals from aqueous solutions using immobilized fungal biomass in continuous mode, *Water Res*. **32** (1998) 1968-1977.

[4] K. Chojnacka, A. Chojnacki, H. Górecka, Biosorption of Cr^{3+}, Cd^{2+} and Cu^{2+} ions by blue-green algae *Spirulina sp*.: Kinetics, equilibrium and the mechanism of the process, *Chemosphere* **59** (2005) 75-84.

[5] W.-Y. Lee, W.-X. Wang, Metal accumulation in the green macroalga *Ulva fasciata*: Effects of nitrate, ammonium and phosphate, *Sci. Total Environ*. **278** (2001) 11-22.

[6] E. Fourest, B. Volesky, Alginate properties and heavy metal biosorption by marine algae, *App. Bio*. **67** (1997) 33-44.

[7] Z.R. Holan, B. Volesky, Biosorption of Cd by biomass of marine algae, *Biotechnol. Bioeng*. **41** (1993) 819-825.

[8] T.A. Davis, B. Volesky, R.H.S.F. Vieira, *Sargassum* seaweed as biosorbent for heavy metals, *Water Res*. **34** (2000) 4270-4278.

[9] M.M. Figueira, B. Volesky, V.S.T. Ciminelli, F.A. Roddick, Biosorption of metals in brown seaweed biomass, *Water Res*. **34** (2000) 196-204.

[10] W. Ma, J.M. Tobin, Development of multimetal binding model and application to binary metal biosorption onto peat biomass, *Water Res*. **37** (2003) 3967-3977.

[11] R.J.E. Martins, R. Pardo, R.A.R. Boaventura, Cadmium(II) and zinc(II) adsorption by the aquatic moss *Fontinalis antipyretica*: Effect of temperature, pH and water hardness, *Water Res*. **38** (2004) 693-699.

[12] A.K. Bhattacharya, C. Venkobachar, Removal of cadmium(II) by low cost adsorbents, *J. Environ. Eng*. **110** (1984) 110-122.

[13] Y.S. Ho, C.C. Wang, Pseudo-isotherms for the sorption of cadmium ion onto tree fern, *Proc. Biochem*. (2003) 1-5.

[14] A. Marques, H.M. Pinheiro, J.A. Teixeira, M.F. Rosa, Removal efficiency of Cu^{2+}, Cd^{2+} and Pb^{2+} by waste brewery biomass: pH and cation association effects, *Desalination* **124** (1999) 137-144.

[15] V.J.P. Vilar, Uptake of metal ions in aqueous solution by algal waste from agar extraction industry, Ph.D. Thesis, Faculty of Engineering University of Porto, Porto, 2006.

[16] V.J.P. Vilar, C.M.S. Botelho, R.A.R. Boaventura, Influence of pH, ionic strength and temperature on lead biosorption by *Gelidium* and agar extraction algal waste, *Proc. Biochem*. **40** (2005) 3267-3275.

[17] V.J.P. Vilar, C.M.S. Botelho, R.A.R. Boaventura, Copper removal by algae *Gelidium*, agar extraction algal waste and granulated algal waste: Kinetics and equilibrium, *Biores. Technol*. doi:10.1016/j.biortech.2007.01.042 (2007).

[18] V.J.P. Vilar, C.M.S. Botelho, R.A.R. Boaventura, Kinetics and equilibrium modelling of lead uptake by algae *Gelidium* and algal waste from agar extraction industry, *J. Hazard. Mater*. **143** (2007) 396-408.

[19] V.J.P. Vilar, C.M.S. Botelho, R.A.R. Boaventura, Chromium and zinc uptake by algae *Gelidium* and agar extraction algal waste: Kinetics and equilibrium, J. Hazard. Mater. doi:10.1016/j.jhazmat.2007.04.023 (2007).

[20] V.J.P. Vilar, O.M.S. Freitas, P.M.S. Costa, C.M.S. Botelho, R. Martins, R.A.R. Boaventura, Cr(III) uptake by algal biomass: Equilibrium and kinetics experiments, *Journal of Environment and Waste Management*, Accepted (2007).

[21] V.J.P. Vilar, F. Sebesta, C.M.S. Botelho, R.A.R. Boaventura, Equilibrium and kinetic modelling of Pb^{2+} biosorption by granulated agar extraction algal waste, *Proc. Biochem.* **40** (2005) 3276-3284.

[22] V.J.P. Vilar, C.M.S. Botelho, R.A.R. Boaventura, Lead and copper biosorption by marine red algae *Gelidium* and composite material in a CSTR ("Carberry" Type), *Chem. Eng. J.* **10**.1016/j.cej.2007.07.059 (2007).

[23] V. Vilar, C. Botelho, R. Boaventura, *Biosorption performance of a binary metal mixture by algal biomass: Column experiments*, in: J.M. Loureiro, M.T. Kartel, Combined and hybrid adsorbents: Fundamentals and applications, NATO science through security series C, Springer, Kiev, 2006, pp. 281-286.

[24] V.J.P. Vilar, C.M.S. Botelho, R.A.R. Boaventura, Copper desorption from *Gelidium* algal biomass, *Water Res*. **41** (2007) 1569-1579.

[25] V.J.P. Vilar, C.M.S. Botelho, R.A.R. Boaventura, Equilibrium and kinetic modelling of Cd(II) biosorption by algae *Gelidium* and agar extraction algal waste, *Water Res.* **40** (2006) 291-302.

[26] M.B. Carver, D.G. Stewart, J.M. Blair, W.N. Selander, A FORTRAN-oriented simulation package for the automated solution of partial and ordinary differential equation systems, *AECL*-**5821**, 1979.

[27] G.F. Froment, K.B. Bischof, *Chemical reactor analysis and design*, John Wiley & Sons, New York, 1990.

[28] M.M. Figueira, B. Volesky, K. Azarian, V.S.T. Ciminelli, Biosorption column performance with a metal mixture, *Environ. Sci. Technol*. **34** (2000) 4320-4326.

[29] B. Volesky, Sorption and biosorption, 1st edition, BV Sorbex, Inc., Quebec, 2003.

[30] J.M. Tobin, J.C. Roux, *Mucor* biosorbent for chromium removal from tanning effluent, *Water Res*. **32** (1998) 1407-1416.